Heat Accumulation Mechanism of the Gaoyang Carbonatite Geothermal Field, Hebei Province, North China

Baojian Zhang[1,2]*, Siqi Wang[1,2], Fengxin Kang[3]*, Yanqiu Wu[4], Yanyan Li[1,2], Jun Gao[1,2], Wenzhen Yuan[1,2] and Yifei Xing[1,2]

[1]Chinese Academy of Geological Sciences, Beijing, China, [2]Technology Innovation Center of Geothermal and Hot Dry Rock Exploration and Development, Ministry of Natural Resources, Beijing, China, [3]Shandong Provincial Bureau of Geology and Mineral Resources, Jinan, China, [4]School of Water Resources and Environment, China University of Geosciences (Beijing), Beijing, China

From 2019 to 2021, we constructed two high-productivity geothermal wells with wellhead temperatures of 109.2 and 123.4°C in the Gaoyang geothermal field. Based on the two wells, it was proved that Gaoyang is a medium-temperature carbonate geothermal field with great development potential. The article reported the latest exploration achievements of deep buried hill geothermal resources in the geothermal field. The productivity of D34 and D35 geothermal wells were evaluated by James end-pressure method: the total flow of steam–water mixture was 234.59–331.92 (t/h), the dryness was 1.36–2.03%, and the single-well power generation potential was 2.10–2.55 MW. Combined with those results, the heat control factors and heat accumulation mechanism of the deep carbonatite geothermal field were confirmed. The westward subduction of the Pacific plate caused obvious damage to the eastern North China Craton and greatly reduced the thickness of the lithosphere and crust. This process facilitated the conduction of mantle-derived heat to shallow crust. Deep strike-slip faults (e.g., Maxi fault) cut through the lithosphere, leading the deep mantle-derived heat and magma to migrate into the crust. The heat accumulated from the depression with low thermal conductivity to the uplift with high thermal conductivity. Groundwater was heated up by deep cycle and convection along faults. The catchment of regional karst groundwater also had a certain effect on the heat accumulation. The Gaoyang geothermal field was formed by these factors.

Keywords: Gaoyang geothermal field, medium-temperature geothermal resources, heat accumulation mechanism, development potential, capacity of geothermal well

1 INTRODUCTION

The study area is within the northeastern Gaoyang geothermal field located in Xiong'an New Area, central Hebei Province. The shallow-seated carbonate thermal reservoirs include the Niutuo and Rongcheng geothermal fields, which are less than 1,000 m, and their development and utilization are simple and large scale with many years of history (Chen et al., 1982). However, the depth of carbonate reservoir of the Gaoyang geothermal field is more than 3,000 m and its development is small scale due to the relatively complex mining technology. The China Geological Survey of the Natural Resources Ministry has conducted a series of exploration and research work of the geothermal resources with the authors to make improvements in this area and has made great progress in the detection of new formations and deep bedrock thermal reservoirs (Wang et al., 2018;

Wu et al., 2018) since the foundation of Xiong'an New Area in 2017. The Chinese Academy of Geological Sciences discovered the highest temperature (123.4°C) geothermal well in the North China basin in 2020 after the foundation of the most productive geothermal well with a temperature of 109.2°C in 2019 in Gaoyang geothermal field. The exploration results show that the geothermal field with medium temperature (>90°C) has great development and utilization potential.

Regarding the heat accumulation mechanism of the ancient buried hill geothermal field in the North China basin, Chen (1988), Chen (1992) has found that the geothermal anomaly in the uplift of the North China basin is triggered by the redistribution of the relatively uniform heat flow in deep crust to the surface during the upward conduction. Pang et al. (2017) propose a new geothermal genesis model (heat accumulation of binary sources) of the Niutuo geothermal field and points out that the abundant geothermal resources in Xiong'an New Area are formed under dual mechanism, that is, rock thermal conductivity and basin-scale groundwater circulation. Yue et al. (2020) summarize the geothermal accumulation of the ancient buried hills in Xiong'an New Area as a four-element (heat conduction, structural uplift, deep fractures, and convection within the reservoir) model by heat conduction simulation (Yue et al., 2020). However, the key issue about how the heat sourced from mantle and deep crust migrated to the shallow crust remains poorly understood. Wang et al. (2017) report that the obvious thinning of the lithosphere, crustal deformation, earthquakes, and magmatic activities caused by the destruction of the North China crust (NCC) have promoted the production of geothermal resources. Wang and Lin (2020) assign the genetic model of geothermal systems in China as "homologous symbiosi-crust and mantle heat generation-tectonic heat accumulation" and point out that the high-temperature subcrust matter can flow up to the shallow crust along deep fractures. Zhang et al. (2020) confirm that the upwelling of deep mantle-derived thermal matter is a favorable factor for the formation of hot dry rocks in Matouying, Hebei Province (Zhang et al., 2020). Wang et al., 2021 comprehensively analyze the heat accumulation mechanism of deep ancient buried hill geothermal resources in the northeastern Gaoyang geothermal field and discuss the controlling effects of the deep geological structure on the heat distribution in the ancient buried hills (Wang et al., 2021).

Based on the earlier discussion, the heat accumulation mechanism of the buried hill geothermal field in the large sedimentary basin is established. It is the redistribution of the relatively uniform heat flow in deep crust to the surface during the upward conduction (Chen, 1988; Chen, 1992). Under the differential effect of rock thermal conductivity, the heat flow accumulates from the depression with low thermal conductivity to the uplift with high thermal conductivity, and the geothermal water heated by deep cycle from the recharge area to the discharge area and the upper crust fracture upwells after undergoing basin-scale groundwater circulation. This type of geothermal resource can be called "low–medium temperature convective–conductive geothermal system" (Wang et al., 2015). The deep-cycle heating of groundwater along faults generally occurred within a depth of 10 km. Therefore, the deep geothermal anomaly caused by the

deep crust or mantle heat upwelling and its activity mechanism is worth further discussion. Based on previous studies, this article reports the latest exploration achievements of geothermal resources in the Gaoyang geothermal field, proposes the heat accumulation mechanism, and estimates its development potential. The productivity and resource potential of Gaoyang carbonate were evaluated. It could provide geological basis and technical support for efficient development and utilization of deep medium-temperature geothermal resources in the Gaoyang geothermal field and elsewhere worldwide with the same geological setting.

2 GEOLOGIC SETTING

2.1 Geological Structure

The study area is located in the middle-west of the Jizhong depression within the Bohai Bay basin. The Jizhong depression is mainly the secondary tilted block, half-graben depression and buried hill structural units, which are composed of a series of normal faults or inverted normal faults formed under Mesozoic compression and Cenozoic extension. The geothermal field has two structural units (the Gaoyang low uplift and the Lixian slope), which are distributed in NE direction strips as a whole. It is separated from the Rongcheng uplift and the Niutuo uplift by the Anxin-Wen'an structural transfer zone in the NWW–SEE direction in the north, and it is connected to the Xingheng uplift by the Hengshui-Wuji structural transfer zone in the NW–SE direction in the south, with the Baoding depression in the west, and the Raoyang depression in the east, respectively (**Figure 1**). The carbonate geothermal reservoir at the top of the Gaoyang uplift is buried at a depth of 3,000–3,500 m and gradually deepens to below 4,000 m in the depressions on the east and west sides, respectively (**Figure 2**).

The main Gaoyang-Boye fault occurs along the axis of the Gaoyang low uplift with NE trending. Its fault distance in the north is relatively small, and the activity is significantly weakened after the Paleogene. However, faults developed in the structural transfer zone at the north and south ends of the geothermal field. The Anxin-Wen'an structural transfer zone is mainly composed of a series of echelon faults such as the Anxin fault and the Niunan fault. "Transfer zone" is derived from the study of the fold-thrust fault in the compression deformation of the Canadian Rocky Mountains, which is an adjustment structure that can enable the amount of shortening is more nearly constant (Dahlstrom, 1970). This concept of transfer zone was later applied to extensional structures and strike-slip structures (Morley et al., 1990; Faulds and Varga, 1998; Qi, 2007; Yang, 2009). Transfer zone is a favorable tectonic regime for formation of oil, gas, and geothermal resources, as its development is of multi-level faults.

The N–S trending Maxi strike-slip fault has gone through weak extensional activities and sedimentation-controlling effect due to the influence of the Anxin-Wen'an structural transfer zone in the north. The fault is part of a large basement strike-slip fault and the Tangshan-Hejian-Cixian fault (Qi, 2004). The Niudong Maxi strike-slip structural system composed of the Maxi fault and
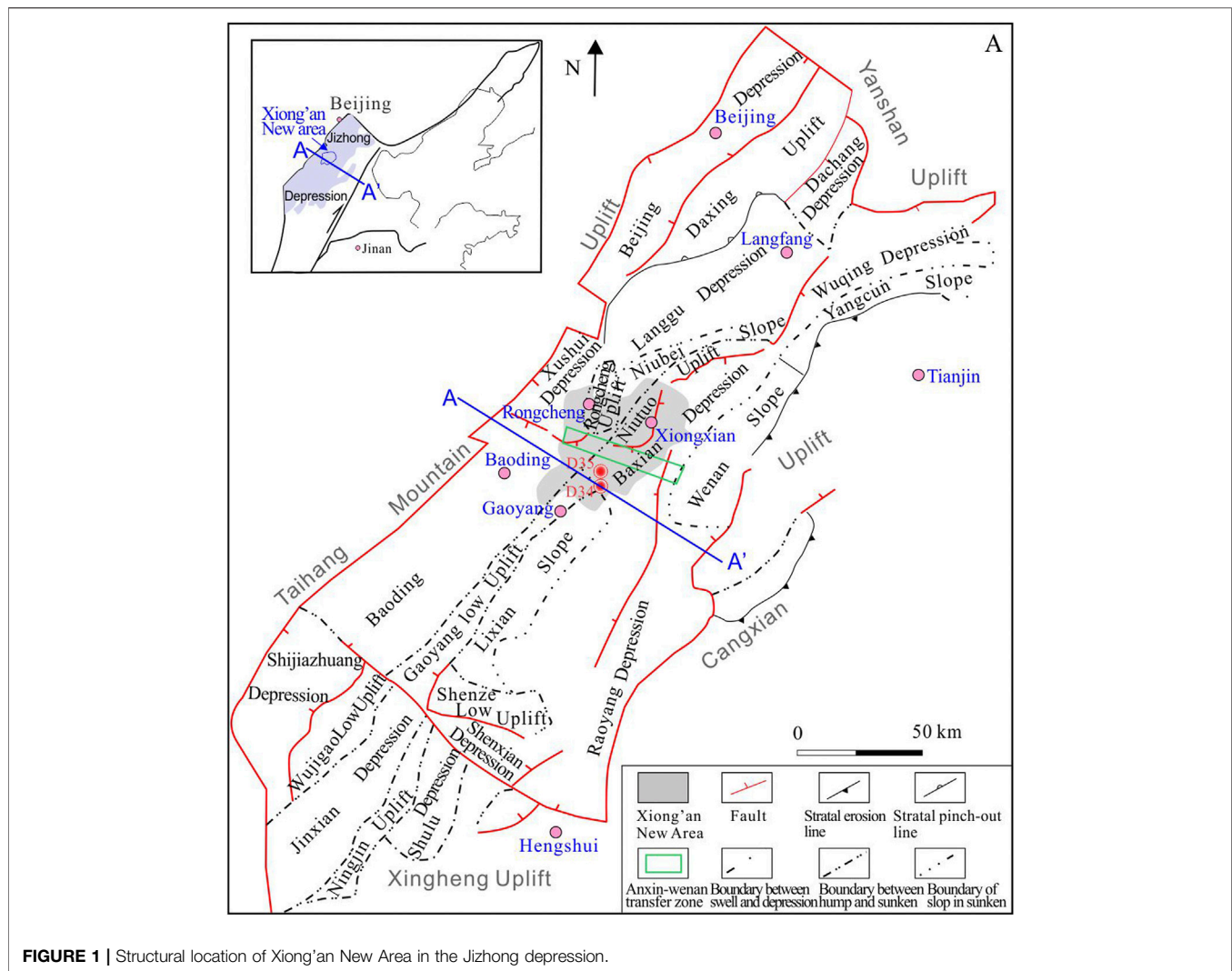
FIGURE 1 | Structural location of Xiong'an New Area in the Jizhong depression.
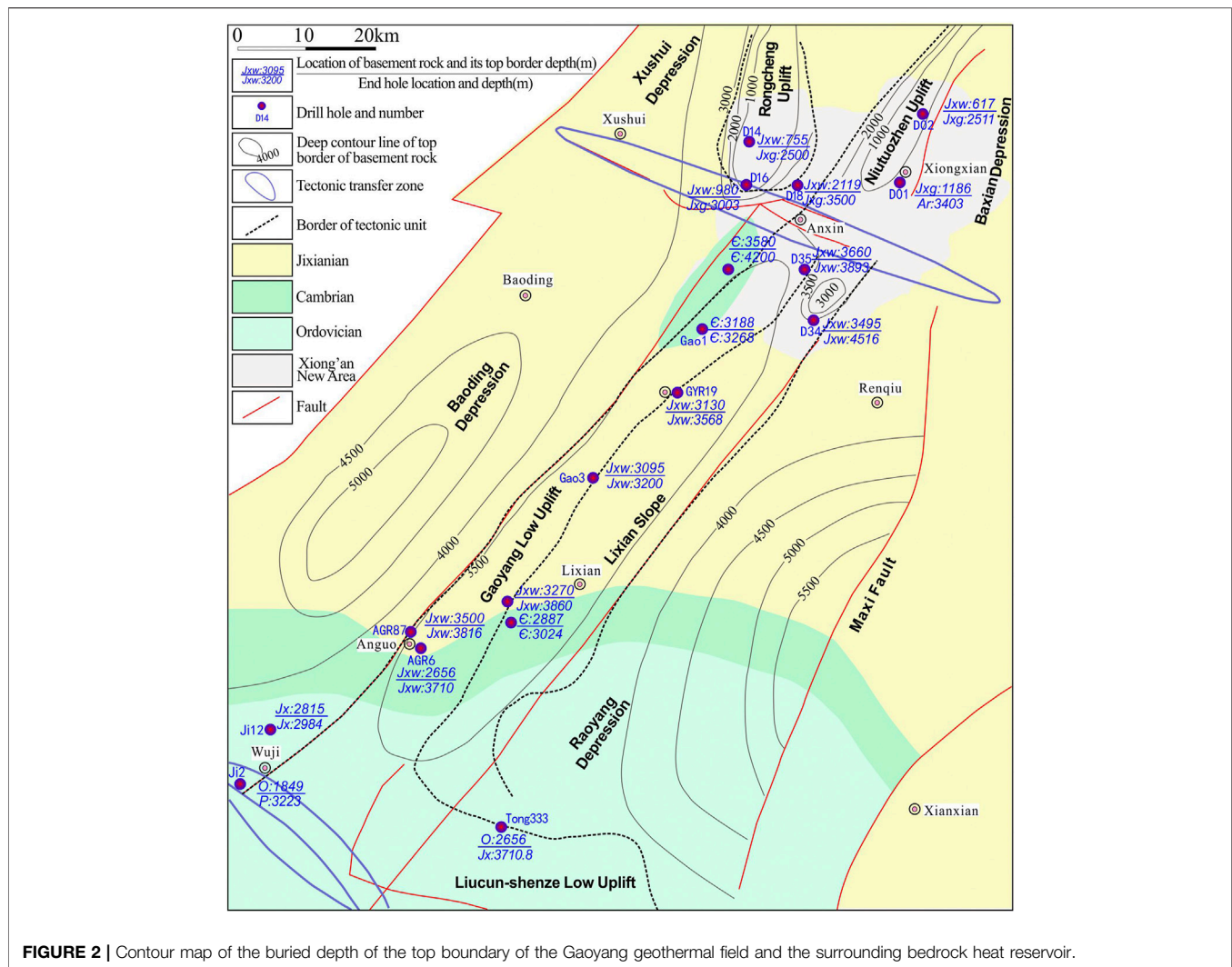
the Niudong fault is considered to be the result of right-lateral strike-slip activities of deep faults that cut through the basement in the Cenozoic. This is direct evidence that deep tectonic stress is transferred to the shallow crust through the lower crust (Xiao et al., 2000).

2.2 Deep Geological Structure

The western Pacific plate subducted to northwest in the Early Jurassic and retreated in the Early Cretaceous. The subduction, rollback, and retreat of the western Pacific plate eventually led to the stagnation of the slab in the mantle transition zone—the big mantle wedge under eastern Asia. This process (craton destruction) may significantly change the physical properties and viscosity of that section and the overlying mantle, resulting in nonsteady flow of the overlying mantle wedge, and may further dramatically give rise to the increase of melt/fluid contents in the lithospheric mantle, lower viscosity, the stretch/decompression of the lithosphere, and the transformation from the old cratonic lithosphere to the young mantle (Zhu and Xu, 2019). Groundwater played an important role in the

destruction of the NCC lithosphere. During the subduction of the plate, a large amount of water was released into the cratonic lithospheric mantle and caused strong hydration. As a result, the mantle convection system in the eastern NCC destabilized and the overlying lithosphere was metasomatized, melted, and weakened, which led to lithospheric thinning and cratonic destruction (Xia et al., 2013).

The thermal erosion *via* mantle convection and peridotite-melt interaction within the big mantle wedge resulted in significant thinning of the NCC lithosphere during the Mesozoic. Due to the retreat of the subducting plate, the lithosphere extended and further thinned, accompanied by the passive upwelling of the asthenosphere, which led to the development of the Bohai Bay sedimentary basin in the Cenozoic as well as the increase in the surface heat flow. In the late Cenozoic, under the effect of thermal attenuation, the lithosphere gradually thickened, but still maintained a thin state and high heat flow (He and Qiu, 2014). As the thickness of the lithosphere changed, the lithosphere of the Bohai Bay basin transformed its thermal structure from "cold mantle but hot
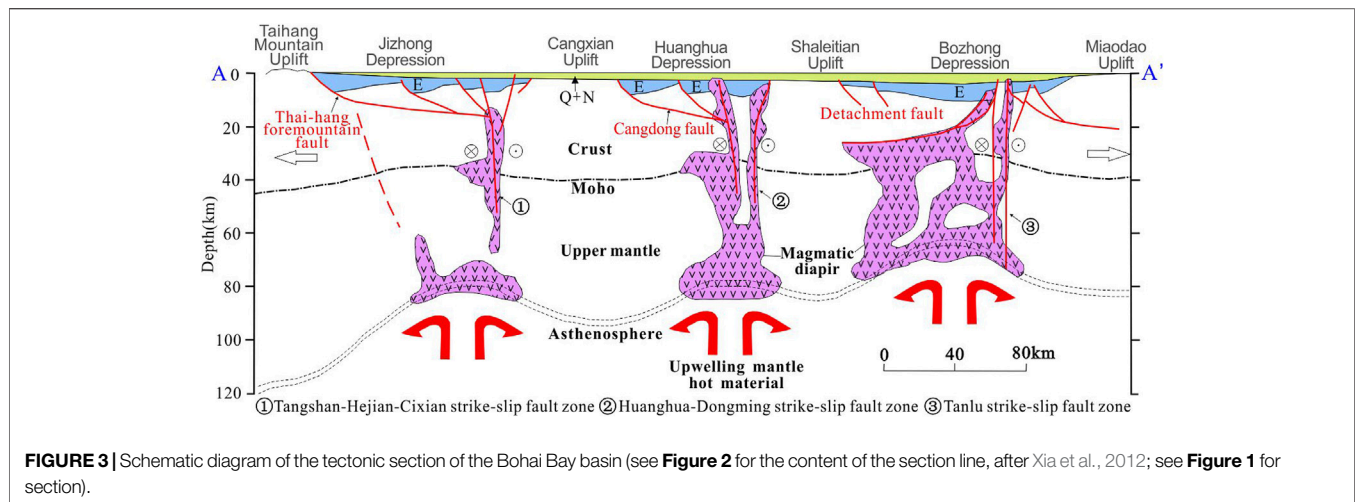
FIGURE 2 | Contour map of the buried depth of the top boundary of the Gaoyang geothermal field and the surrounding bedrock heat reservoir.

crust" in the Triassic–Jurassic to "hot mantle but cold crust" stage in the Cretaceous–Cenozoic (Zuo et al., 2013). It can be concluded that thermal erosion is a factor deduced from the thinning of the NCC lithosphere. The thinning of the lithosphere made the eastern NCC at a high degree heat flow (60–68 mW/m^2).

2.3 Neotectonics and Its Dynamic Mechanism

Neotectonic movements are not well developed in the study area, whereas the Maxi fault in the eastern Raoyang depression is a large strike-slip fault in the Cenozoic, which is a part of the Tangshan-Hejian-Cixian active tectonic zone. It is a new-born seismotectonic zone consisting of the Cixian-Handan fault, Xinhe fault, Tangshan fault, and Maxi fault. Most of them are right-lateral normal with NE trending. The earthquakes in this area are strong today. About 4 M > 7.0 earthquakes were recorded, including the 1966 Xingtai M7.2 earthquake and the 1976 Tangshan M7.8 earthquake. The focal rupture is dominated by

the right lateral strike-slip fault, and a steep dip was formed during the process (Xu et al., 1996).

Neotectonic movements in North China are controlled by the interaction of two lithospheric structures, that is, the far-field effect of India–Eurasia collision and the upwelling of lithospheric mantle. First, the eastward push in the northeastern Qinghai–Tibet resulted in compressional and strike-slip deformation occurring along the Tanlu fault zone in the eastern North China. Furthermore, the upwelling of deep mantle caused by the subduction of the Pacific plate dominated regional thermal subsidence and Quaternary mantle-derived volcanic activity in the eastern North China. These two lithospheric tectonic forces alternated in time and space, controlling the differential evolution history of neotectonic landforms in North China (Zhang et al., 2019). The surface crust is mainly controlled by the collision and push of the Indian plate, while the deep crust is affected by the westward subduction of the Pacific plate, providing an energy source for shallow movement and controlling super-large earthquakes on the surface. The regional deep strike-slip faults constitute the main channels

FIGURE 3 | Schematic diagram of the tectonic section of the Bohai Bay basin (see **Figure 2** for the content of the section line, after Xia et al., 2012; see **Figure 1** for section).

for the upwelling of the mantle heat (Xia et al., 2012; **Figure 3**). The high heat flow zone is closely related to the distribution of deep basement faults (Zuo et al., 2014).

2.4 Features of Geothermal Reservoir

The main strata of the Gaoyang geothermal field are Archean, Changcheng, Jixian, Cambrian, Ordovician, Paleogene (in depression and low uplift), Neogene, and Quaternary. The thermal reservoirs are mainly composed of the Jixian Wumishan, Changcheng, and Gaoyuzhuang formations. Above the Wumishan Formation, there is a thin Cambrian–Ordovician reservoir in the south of the geothermal field.

2.4.1 Jixian Wumishan Formation Reservoir

The Jixian Wumishan Formation reservoir consists of dolomite rocks located on the top of the Gaoyang low uplift and the Yanling buried hill in the northern Lixian slope. The depths of the top boundary and low boundary are 3,000–3,500 m and 3,500–4,000 m, respectively. The thickness of the Wumishan Formation is about 1,000–1,400 m, and the average thickness ratio is about 19%. The rock porosity is generally less than 6%, and the maximum and the average are 22.4% and 3.39%, respectively. The permeability ranges from 0.01 to 1,000 mD, most (87.8%) distributed between 0.01 and 100 mD (Dai et al., 2019). The depth of D35 is 3,853 m, revealing 218.5 m of the Wumishan Formation reservoir (not penetrated). The main lithology is gray-white and light gray dolomite rocks with argillaceous. The lower segment contains blue-gray, brown intrusive diorite porphyrite and structural breccia, and the upper segment is highly weathered with well-developed fractured karst. The thickness of the fractured aquifer is 43 m, accounting for 19.68% of the formation.

2.4.2 Changcheng–Gaoyuzhuang Formation Reservoir

Several wells were drilled to the Changcheng–Gaoyuzhuang Formation with thickness over 1,000 m in the study area. The lithology is dominantly gray dolomite intercalated with argillaceous and siliceous dolomite with flint. The porosity is 2–6% and with permeability varying from 0.1 to 160 mD. The

temperature of the formation is generally around 75–95°C. The yield and TDS of well water are ~45–80 m^3/h and 3,000 mg/L, respectively. The depth of D34 is 4,507.43 m, revealing 814.43 m of the Changcheng–Gaoyuzhuang Formation (not penetrated). The main lithology is gray and off-white dolomite rocks with a lot of flint and a small amount of calcite particles and quartz. The overlying Yangzhuang Formation (209.19 m) and Wumishan Formation (29 m) are composed of purple-red and off-white gravel-bearing dolomite rocks and off-white dolomite, respectively. The thickness of the fractured aquifer in the Gaoyuzhuang Formation is 173 m, accounting for 21.24% of the total formation.

2.4.3 Cambrian–Ordovician Reservoir

The Cambrian–Ordovician reservoir is mainly distributed in Anguo-Boye-Lixian-Anping on the southern Gaoyang geothermal field. The top boundary has karst fissures with a depth of 2,800–3,500 m. The Ordovician Formation accounts for 32% in total reservoir thickness, whereas the ratio of Cambrian Formation is 16.5%. AGR50 reveals 460 m of the Cambrian reservoir, and the depth of the top boundary is 3,000 m.

The top boundary of the Jixian Formation in the buried hill of Anxin-Wen'an transfer zone is buried at a depth of 2,500–3,500 m and the depression bedrock with a depth more than 4,000 m. While outside the study area, the depth of the depression bedrock can reach to 5,000 m. The maximum depth of the bedrock in the Raoyang depression is more than 6,500 m, and that in the Baxian depression is above 10,000 m. The Anxin-Wen'an transfer zone is the direction of fluid (oil and gas) migration and a favorable place for fluid (oil and gas) accumulation in the Raoyang depression and Baxian depression.

3 METHODS

3.1 Deep Geological Structure

For analyzing the upwelling of hot materials from the mantle or deep crust and the influence of their activity mechanism on the deep geothermal anomaly, the deep geological structure of the

study area is researched. We collected previous magnetotelluric soundings and artificial seismic soundings of the study area (Liu and Liu, 1982; Dai et al., 1995; Lu et al., 1997; Xu 2003) to determine the depth of the asthenosphere and the undulation shape of the top surface and Moho surface of the circle. The multilayer structure, the interlayer active surface, and the active structure of the crust in the study area are further identified and the upwelling mechanism and channel of deep thermal materials analyzed.

3.2 Method of Correction of Earth's Heat Flow

Heat flow refers to the heat transferred from the interior of the earth to the surface by heat conduction per unit area and unit time and then dissipated into space. Under one-dimensional steady-state conditions, the heat flow is the thermal conductivity of the rock and the vertical temperature product of gradients (Lin W. J. et al., 2021).

Based on the Fourier's law, the heat flow value was calculated by multiplying the geothermal gradient with the thermal conductivity value (**Eq. 1**) (Bullard and Schonland, 1939). The surface heat flow value can also be calculated by combining the basal heat flow value at the bottom of the formation with the heat flow value contributed by radiogenic heat production within the overlying formation (**Eq. 2**) (Morgan, 1984).

$$Q = \lambda \frac{dT}{dZ} \qquad (1)$$

$$Q_b = Q_0 - A \cdot \Delta Z \qquad (2)$$

where Q is the heat flow in $mW \cdot m^{-2}$, dT/dZ is the temperature gradient in $^\circ C \cdot km^{-1}$, λ is the thermal conductivity, Q_b and Q_0 are the heat flows at the bottom and top of the formation, ΔZ is the formation thickness in km, and $A \cdot \Delta Z$ is the heat flow value, which was contributed by the overlying formation.

The "baking" effect of higher-temperature hot water formed by hydrothermal convection from deep dolomite geothermal reservoirs and the influence of lateral convergence of heat flow on regional normal heat flow needs to be eliminated. Based on the heat transfer due to the heat flow of the metamorphic bedrock layer in Well D01 and the heat flow values generated by the heat generation rate of the upper rock layer, combined with the formation information of different wells in the study area and the heat generation rate data of different rock layers, the heat flow value in the Xiong'an New Area is recalculated, to analyze and evaluate the size of the real heat flow value in this area (Wang et al., 2021).

3.3 Test of Productivity on Geothermal Storage

For evaluating the productivity of the D34 and D35 geothermal wells, a high-temperature and high-pressure well test experiment was conducted in this research. The working pressure of the pressure sensor is 0–100 MPa, and the working temperature is 0–150°C. When it is put down to 350 m depth of the well, the probe records the pressure and temperature every 10 s. Then the

probe is raised and the data are read (**Figure 4**). The pressure and temperature of the three trips are verified with the manually measured water level. After pumping, the end pressure is tested at the discharge port with a pressure gauge installed at the wellhead. Compared with the manually measured temperature, pressure, and flow data, the errors are all within 3%, indicating that the obtained data are accurate. The total flow and steam flow of the mixture were roughly calculated using the James end-pressure method.

The productivity parameters of D34 and D35 geothermal wells constructed in this research are shown in **Table 1**. Combined with the data of the surrounding carbonate geothermal wells, the wellhead temperature of the carbonate geothermal wells buried below 4,500 m is generally 95–120°C, with the bottom hole temperature being 105–140°C of the Gaoyang geothermal field. It is assigned to the middle-temperature geothermal resources. The total flow of the steam–water mixture in a single well is 234.59–331.92 t/h, the steam flow is 4.51–4.76 t/h, the dryness is 1.36–2.03%, and the single-well power generation potential is 2.10–2.55 MW, which has a good development potential.

3.4 Comprehensive Logging

For obtaining the porosity, permeability, and other aquifer properties of the carbonate geothermal reservoirs of D34 and D35, full hole logging is carried out by SKD-3000B numerical control logging tool. The logging items include well temperature, well diameter, well deviation, resistivity, natural potential, natural gamma, and time difference of acoustic wave. The average relative errors of natural gamma ray, 2.5 m gradient resistivity, and 0.5 m potential resistivity are 4.5, 4, and 4.5%, respectively. All the logging quality meets the specification requirements. The logging data are processed by forward exploration logging interpretation platform.

According to the results of logging interpretation and core logging, it is concluded that the geothermal reservoir of D34 is mainly Gaoyuzhuang Formation of Jixian and that of the D35 is mainly Wumishan Formation. The performance parameters of the geothermal reservoir aquifer of the geothermal well are shown in **Table 2**. The logging results show that Wumishan and Gaoyuzhuang formations on the depth of the study area are carbonate geothermal reservoir aquifers with fracture karst or karst fractures, with relatively developed voids and strong permeability, which ensure the high productivity of Jixian system geothermal reservoir in deep depth. Among them, the well temperature is measured after standing for 120 h after the well test, for ensuring steady-state well temperature data. According to the well temperature measurement results, the steady-state temperature measurement curve of geothermal well is drawn (**Figure 5**).

4 RESULTS AND DISCUSSION

4.1 Heat Control of the Lithosphere, the Moho Uplift

The Pacific plate subducted westward in the Early Jurassic and subducted toward the NW low-angle plate in the Late Jurassic–Early Cretaceous (~170 Ma), causing the subduction

FIGURE 4 | Well test equipment: **(A)** CEP2 high-temperature probe; **(B)** end-pressure gauge; **(C)** thermometer; **(D)** flow meter.

TABLE 1 | Parameters of geothermal well thermal reservoir capacity evaluation of D34 and D35.

No.	Formation of water intake	Depth of water intake (m)	Wellhead temperature (°C)	Average temperature of geothermal reservoir (°C)	Diameter of discharge pipe (cm)	End pressure of discharge pipe (bar)	Total flow of steam–water mixture (t/h)	Steam flow (t/h)	Dryness (%)	Power generation potential of single well (MW)
D34	Gaoyuzhuang	3,458.78–4,507.43	123.4	133	15	2.2	234.59	4.76	2.03	2.10
D35	Wumishan	3,660–3,853	109.2	116	15	3.1	331.92	4.51	1.36	2.55

TABLE 2 | Properties of aquifer in the carbonate heat reservoir.

No.	Hydrothermal reservoir	Aquifer thickness (m)	Space form	Porosity (%)	Mean of porosity (%)	Permeability (mD)	Mean of permeability (mD)
D34	Gaoyang Formation of Jixian	10–57	Karst fissure	1.29–3.49	1.81	0.11–1.56	0.33
D35	Wumishan Formation of Jixian	2.3–8.30	Karst cave, solution crack	1.85–7.20	3.93	0.24–9.93	3.16

zone to migrate to the interior of the North China Craton (Ling et al., 2009; Ling et al., 2013). The massive thinning of the lithosphere caused by the NCC destruction has been confirmed based on large amounts of geophysical exploration results. Driven by the subduction of the western Pacific plate, the asthenospheric molten material moved to both sides, causing

FIGURE 5 | Temperature measurement curve of D34 and D35 (G = gradient; °C/100 m).
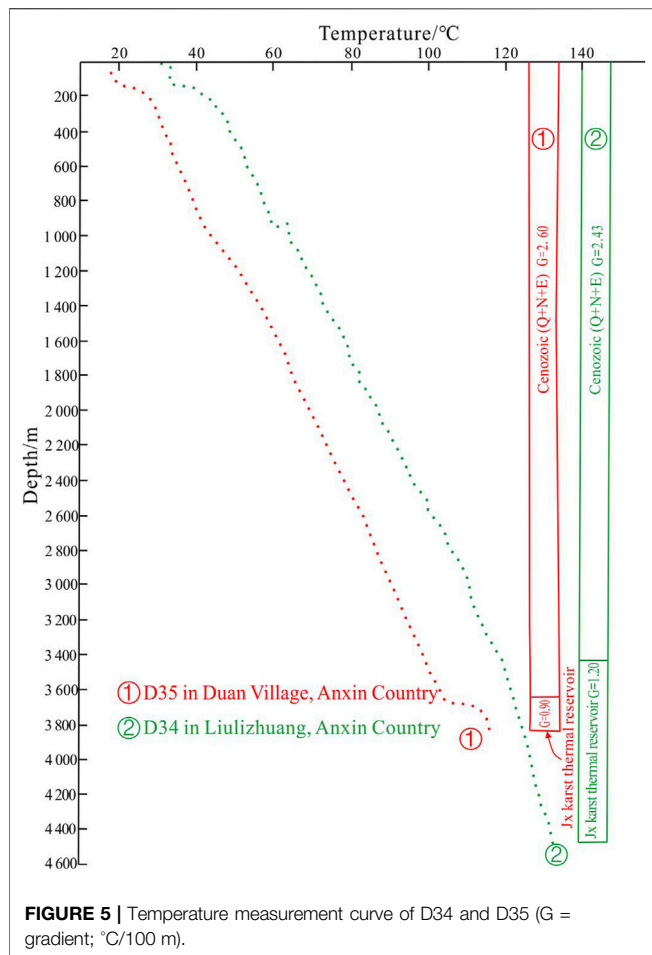
obvious damage to the eastern NCC. In the eastern NCC, the Moho depth is 33 km, and the lithosphere and the crust are significantly thinner than in the central and western NCC. The massive thinning of the lithosphere promotes the conduction of mantle-sourced heat and facilitates deep thermal energy to enter the shallow crust (Wang et al., 2017).

According to the research of Liu and Liu (1982), it can be concluded that the depth of the top surface of the asthenosphere is the consistent position of the high-conductivity layer on the mantle and the low-velocity zone in earthquake. Due to the upwelling of the asthenosphere caused by the destruction of the North China Craton, the lithosphere in the Bohai Bay Basin is obviously thinner, and the lithosphere in the Jizhong depression is thinned to 50–70 km (**Figure 6A**), which is more than 10 km thinner than the surrounding uplift. At the same time, the thickness of the Moho surface in the Jizhong depression is reduced to 32 km, which is 2–4 km thinner than the surrounding uplift (**Figure 6B**). It can be recognized that there is a clear mirror image relationship between the large depression basement and the Moho uplift (Dai et al., 1995; Xu 2003), which means that the asthenosphere and the Moho uplift, the uplift of high-conductivity and low-velocity layers in the crust, the differential movement in the fault block, the basement fault, the strong magma, and other deep activities are relatively well

developed in areas with thinner lithosphere. Therefore, the heat flow and temperature of the depression are higher than that of the uplift at the same depth below the Heat Flow Equilibrium Line.

4.2 Upwelling and Pathways of Deep Heat

Driven by the subduction of the western Pacific plate in the Early Jurassic, a large amount of slab fluid or melt was released into the overlying mantle wedge (**Figure 7A**). During the Early Jurassic, the Paleo-Pacific plate subducted westward and then turned into a low-angle northwestward flat plate subduction in the Late Jurassic–Early Cretaceous (∼ 170 Ma), causing the subduction zone to migrate into the NCC (Ling et al., 2009; Ling et al., 2013), and large amount of slab fluid or melt was released into the overlying mantle wedge (**Figure 7A**). The retreat of the subducted plate in the Early Cretaceous (~130 Ma) caused large amounts of asthenospheric mantle upwelling, which induced the formation of large-scale intraplate magma with high oxygen fugacity (fO_2) (**Figure 7B**). The subduction and retreat of the western Pacific plate caused the asthenospheric heat upwelling in the eastern NCC, reaching the top of the upper mantle and intruding into the crust along the existing supercrust faults (such as the Maxi fault), which resulted in the dehydration of hydrous minerals in the upper mantle and lower crust to produce fluids. From previous studies, the water content of the mantle below the NCC exceeded 1,000 ppm at about 120 Ma and was significantly higher than that of other cratons during the same period, which in turn may have led to the formation of low-velocity and high-conductivity layers in the crust and upper mantle (Xia et al., 2013).

The crust of the Jizhong depression basement has a multilayer structure and interlayer active surfaces, which can generally be divided into high-velocity and low-conductivity upper crust, low-velocity and high-conductivity middle crust, and high-velocity and low-conductivity lower crust (**Figure 8**), evidenced by artificial seismic and magnetotelluric sounding data. The high-conductivity layer is about 15–22 km deep between the middle and lower crust and it is also the location of the deep interlayer sliding surface. The shallow normal faults mostly end in this low-velocity zone (Liu et al., 1984; Lu et al., 1997). Seismic sources mostly occur at the bottom of the upper crust and in the low-velocity middle crust, whereas medium-strong earthquakes mostly occur near the top of the low-velocity middle crust. This indicates that the low-velocity and high-conductivity layer of the middle crust is tectonically active, which is conducive to connect the mantle heat and become a channel for the upwelling of deep mantle-derived heat by cooperating with the deep faults that cut through the crust and even lithosphere. The upwelling geothermal fluids and eruption magma along the deep faults are the main controlling factors for the formation of deep linear (stripe) and beaded thermal anomalies. At the same time, the upwelling mantle-derived heat can also promote the activation of deep fractures or the formation of new fractures and upwelling other heat (Zhang et al., 2020). The characteristic of He isotope of gas reservoirs in the Hejian section of the Maxi fault has an anomalous zonal distribution (R/Ra>1) (Dai et al., 1995), indicating that mantle-derived material may migrate to the shallow crust along the Maxi fault. The contribution of mantle-derived He is between 5 and 8%,
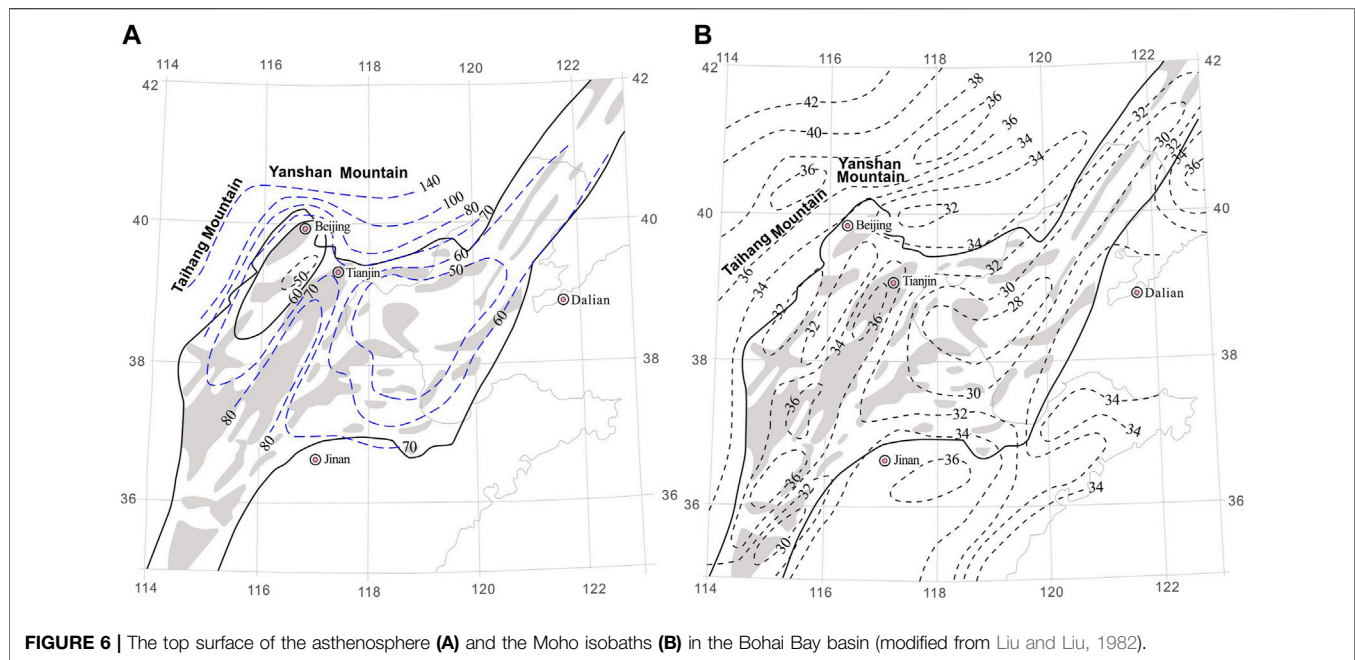
FIGURE 6 | The top surface of the asthenosphere **(A)** and the Moho isobaths **(B)** in the Bohai Bay basin (modified from Liu and Liu, 1982).

showing that deep faults are regional heat-controlling structures and channels for deep fluid convection into shallow reservoirs (Pang et al., 2018). The D34 and D35 have relatively high temperature, which are 20 km away from the Maxi fault. Furthermore, the Anxin-Wen'an structural transfer zone has faults that directly intersect the Maxi fault, which is conducive to connect deep heat sources.

4.3 Distribution of Heat Flow in the Shallow Crust

4.3.1 Heat Control of the Uplift and the Depression

As the thermal conductivity of the bedrock in the uplift is significantly higher than that of the Cenozoic sediments in the depression, the uplift and depression are favorable for distribution and redistribution of heat flow (Xiong and Zhang, 1984; Chen, 1988). Therefore, the deep heat flow is more likely to accumulate to the uplift with high thermal conductivity. The Niutuo geothermal field is well known because of its shallow geothermal anomaly formed by a high geothermal gradient. However, it is just for the shallow crust. For the deep crust, the heat flow accumulates from the depression to the uplift below the horizontal Heat Flow Equilibrium Line (Xiong and Gao, 1982), and above the line when the trend of the accumulation is opposite. Mao (2019), Mao (2018) also studied temperature distribution characteristics and controlling factors in geothermal field and referred to the phenomenon similar to the Heat Flow Equilibrium Line as the High Conductivity Homogenization Depth (Mao, 2019; Mao, 2018). The reasons for this phenomenon may be as follows: first, the thinner lithosphere in the depression is conducive to the upward conduction of deep heat sources; second, deep strike-slip faults tend to spread along the bottom of the depression, which

is conducive to the deep heat upwelling; third, the thermal conductivity of the Cenozoic loose sediments in the depression is lower than that of the base rock in the uplift. These factors cause the temperature at the bottom of the Cenozoic to be significantly higher than that of the uplift at the same depth. The thickness of the Cenozoic is more than 5,000 m in the Baoding depression in the western Gaoyang geothermal field, more than 6,000 m in the Raoyang depression in the east, and can reach to 10,000 m in the Baxian depression in the northeast. As a result, the temperature at the bottom of the Cenozoic around the Gaoyang geothermal field is maintained at 130–300°C and makes it a stable heat source for continuously heating the carbonate reservoirs in the Gaoyang geothermal field.

Combined with the basic heat flow values in the metamorphic rock of well D01 and the heat flow values contributed by the radiogenic heat production of the overlying strata, the surface heat flow values of the Xiong'an New Area were recalculated and the heat flow contour map was drawn (**Figure 9**). It can be seen from **Figure 9A** that before the heat flow correction, the calculated terrestrial heat flow values of the Niutuozhen uplift are significantly higher than those of the Rongcheng uplift and Gaoyang uplift, and the terrestrial heat flow values of the Rongcheng uplift is significantly higher than those of the Gaoyang uplift. These are mainly caused by the difference in thermal conductivity, which leads to the lateral accumulation of the depression area and the section with a large burial depth of carbonate geothermal reservoir to a high bulge with a small thermal storage burial depth. **Figure 9B** shows that the corrected heat flow of the Gaoyang uplift is slightly higher than that of the Niutuozhen uplift and the Rongcheng uplift, which is mainly due to the larger thickness of the Cenozoic in the Gaoyang uplift. The Rongcheng uplift is mainly metamorphic
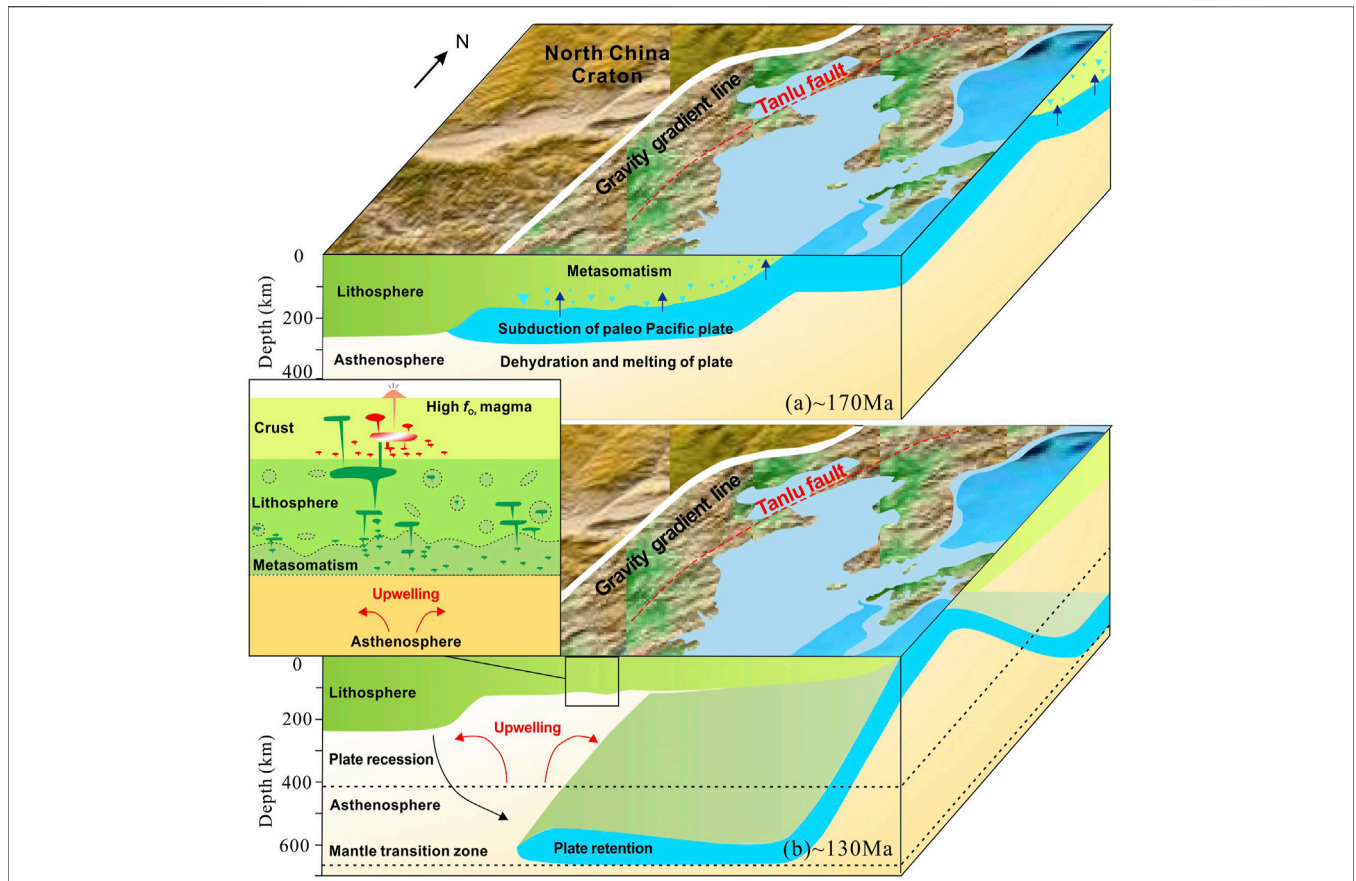
FIGURE 7 | The upwelling mechanism of the mantle-derived thermal material caused by the subduction and retraction of the Paleo-Pacific plate. **(A)** The subduction of the Paleo-Pacific plate may have started in the Early Jurassic. Northwestward flat subductions began in the Late Jurassic to Early Cretaceous, which may have reached the inner land and was responsible for the destruction of the NCC (Ling et al., 2009, 2013). Much slab fluid and melt releases into the overlying mantle wedge. **(B)** The retreat of the (Paleo)-Pacific plate resulted in the upwelling of the asthenospheric mantle and triggered the formation of large-scale high fO$_2$ intraplate magmas.
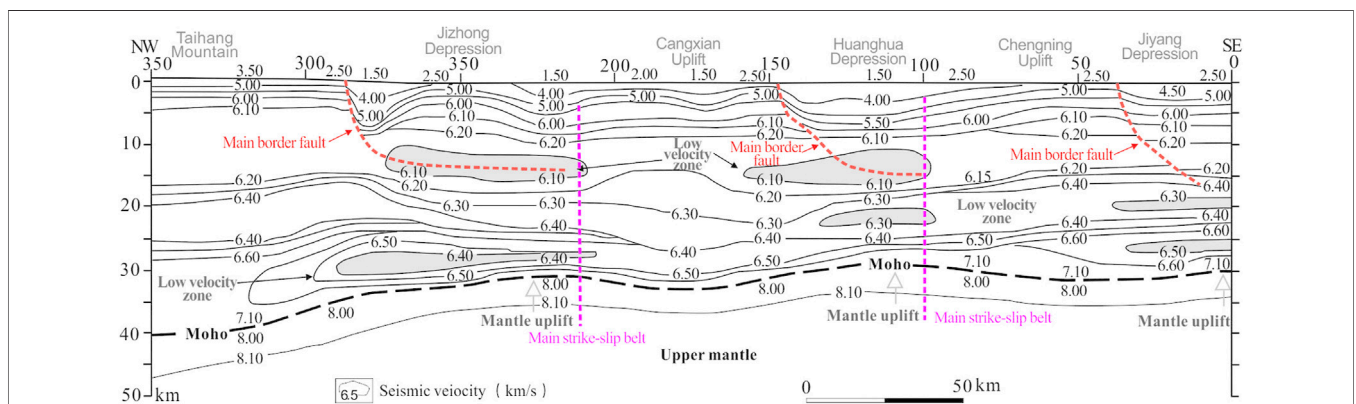
FIGURE 8 | Sectional view of the deep structure in North China (according to Liu et al., 1984).

rocks below the depth of 3,000 m, while the Gaoyang uplift still has carbonate geothermal reservoir of about 1,000 m, and there is still a certain degree of deep circulation convection of hot water.

Numerous concealed basaltic rocks are developed in the Jizhong depression (Wang et al., 2012), and hypabyssal intrusive rocks are distributed in the uplift and the

FIGURE 9 | Comparison of the heat flow map before (A) and after correction (B) (according to Wang Z. et al., 2021).

FIGURE 10 | Contour map of the phreatic pressure level elevation in the Jizhong depression (according to Yan and Yu, 2000).
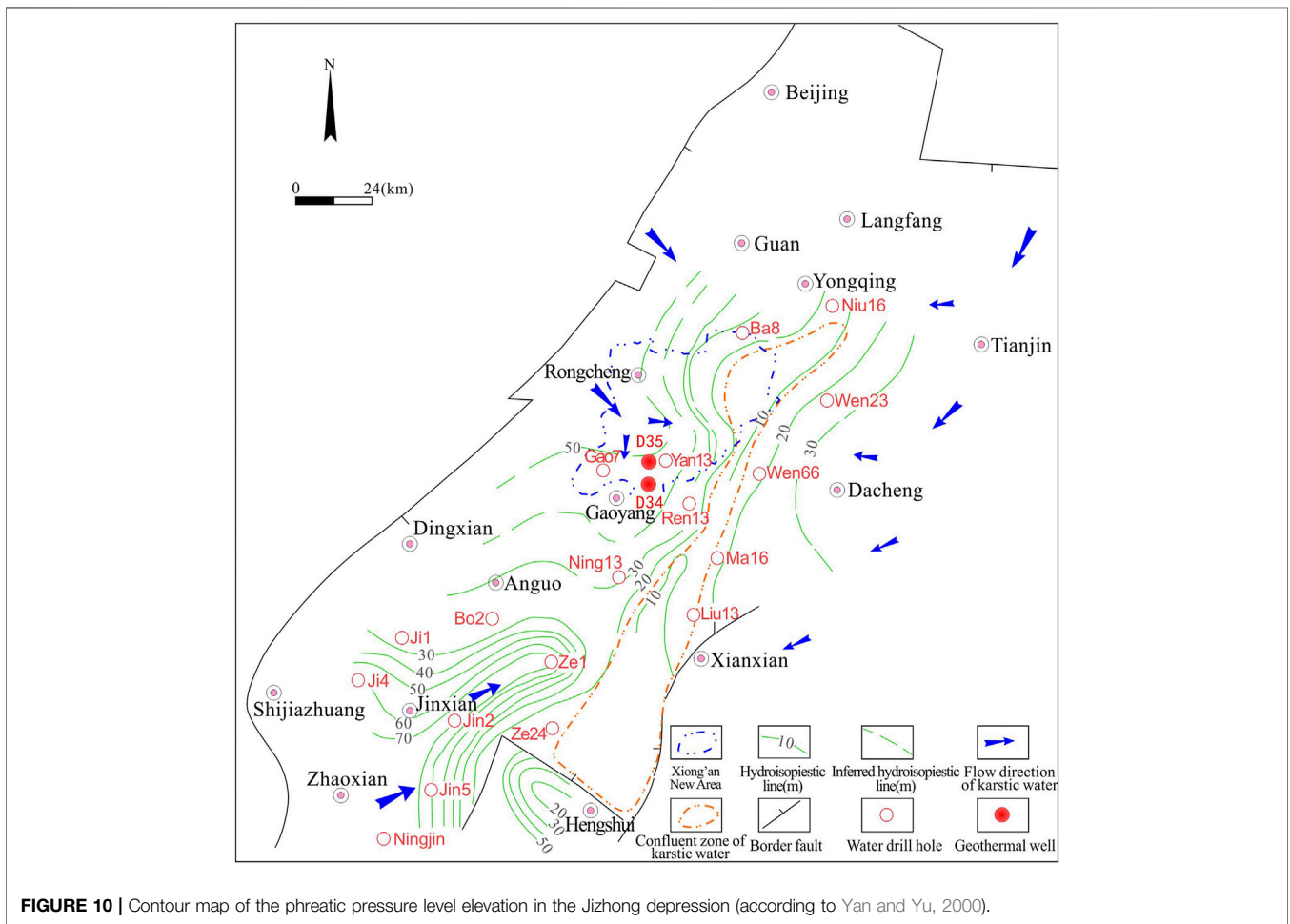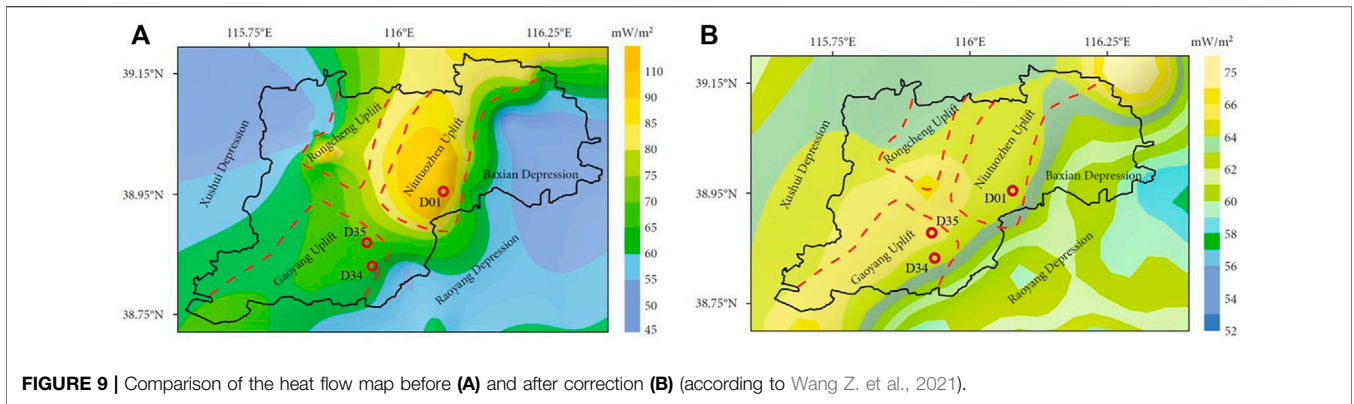
depression in the study area. This area is dominated by Paleogene intrusive rocks. According to the research about D19 in the northwestern Anxin, it is confirmed that the 120 m thick metamorphic basalt is exposed below 3,000 m, and a small amount of blue-gray, brown intrusive diorite porphyry in the Wumishan Formation is also exposed in the lower interval of D35. Although the residual heat retained by early magmatic activities is very small, basalt and diorite porphyry with low thermal conductivity reduce the upward conduction of heat flow. Large-scale layered intrusive rocks can form a "cotton" effect, which makes local geothermal anomalies.
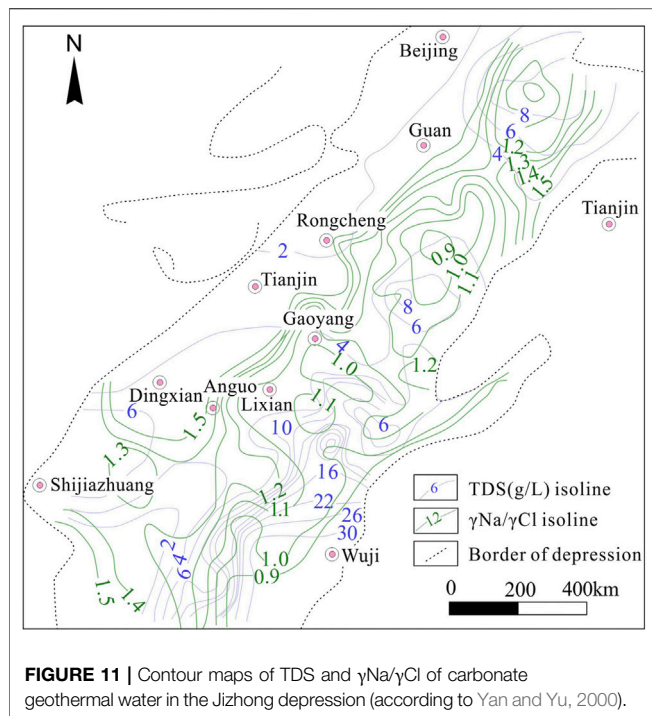
FIGURE 11 | Contour maps of TDS and γNa/γCl of carbonate geothermal water in the Jizhong depression (according to Yan and Yu, 2000).

4.3.2 Deep Circulation Convection Heating of Groundwater Along Faults

Fault structures and caprock conditions also strongly control the accumulation and dissipation of subsurface heat (Lin W. et al., 2021). The faults in the study area control the development of karst and karst paleomorphology. Structural rupture and deformation produce cracks and fractures, forming storage spaces and seepage channels for heat reservoirs. The fractures and faults are conducive to groundwater activity and development of dissolution pores and karstification and finally form a pore–cavity–fracture system. The fault structures and karsts facilitate the groundwater rise after being heated by deep circulation and convection in carbonate rocks, making it easier for deep heat sources to reach the shallow crust to form local shallow thermal anomalies. Therefore, these fault zones are often the areas with well-developed heat reservoirs (Dai et al., 2019). The Cenozoic geothermal gradient (about 2.5°C/100 m) is significantly higher than that of the Jixian carbonate rocks (about 1.0°C/100 m) (**Figure 5**), indicating that the deep circulation and heat convection of groundwater in carbonate rocks below 3,500 m is still relatively strong. The development of fault in the study area provides a channel for the deep circulation heating of carbonate groundwater.

4.3.3 Influence of Hydrodynamic Field on Geothermal Field

Decades of geothermal water exploitation history and the influence of oilfield water injection activities have caused significant changes in the geothermal hydrodynamic field of bedrocks in and around Xiong'an New Area. The present geothermal water hydrodynamic field can no longer reflect the geothermal water recharge, runoff, and discharge conditions in

the bedrocks' natural state. Therefore, we use the earlier hydrodynamic field characteristics (Yan and Yu, 2000) to illustrate the bedrock geothermal water recharge, runoff, and discharge conditions.

The bedrock geothermal water in the Jizhong depression is mainly recharged from Taihang Mountains in the west of the study area and Yanshan Mountains in the north (**Figure 10**). The groundwater level of bedrocks in the Anxin-Wen'an structural transfer zone is slightly higher than that in the uplift on the northern and southern sides. This may be due to a series of NWW–SEE faults in the Anxin-Wen'an structural transfer zone connecting the piedmont faults on the eastern foot of Taihang Mountains, making it easily recharge from the piedmont of Taihang Mountains. The Cangxian uplift is connected to the Yanshan Mountains in the northeast. The karst fissures of shallow carbonate reservoirs are developed and the recharge conditions are better. As a result, the groundwater level of bedrocks in the Cangxian uplift is significantly higher than that in the Jizhong depression on the western side. At the same time, the relatively shallow bedrocks in the Anxin-Wen'an structural transfer zone (the maximum depth is about 5,000 m) are favorable for groundwater derived from the Cangxian uplift to migrate west along the Anxin-Wen'an structural transfer zone. Groundwater from the east and west forms a hydrodynamic balanced zone on the western Renqiu (Zhang et al., 2015) and then flows slowly to the Raoyang and Baxian depressions on the northern and southern sides. In the southeastern Raoyang depression and the western Baxian depression, two confluence centers of regional bedrock groundwater (low potential areas) are formed under the condition of slow movement of groundwater, and heat accumulates to form high-temperature areas. The northeastern Gaoyang geothermal field is close to these two confluence areas, so its temperature is also high.

Contours of total dissolved solids (TDS) and metamorphic coefficient (γNa/γCl) of carbonate geothermal water in the Jizhong depression (Wang et al., 2010; **Figure 11**) show that the TDS in the southeastern Raoyang depression is above 10 g/L, and the metamorphic coefficient is lower than 0.90. TDS in the western Baxian depression is above 6 g/L, and the metamorphic coefficient is lower than 1.0, which respond well to the confluence center of the regional carbonate geothermal water. TDS of D35 is 2.6 g/L, and the metamorphic coefficient is 1.19. TDS of D34 is 2.98 g/L, and the metamorphic coefficient is 1.16. Refer to the carbonate geothermal hydrochemistry data in the Niutuo and Rongcheng geothermal fields; the closer to the confluence area of carbonate geothermal water, the larger the TDS and the lower the metamorphic coefficient, which are more conducive to heat accumulation.

4.4 Heat Accumulation Mechanism

Overall, the heat accumulation mechanism of the Gaoyang medium-temperature geothermal field can be summarized as follows (**Figure 12**). Affected by the westward subduction of the Pacific plate, the eastern NCC was significantly damaged, and the thickness of the lithosphere and crust was greatly reduced. The Moho surface obviously uplifted at the bottom of the depression, which caused the upwelling of asthenospheric

FIGURE 12 | Heat accumulation model of deep ancient buried hill in the northeast of the Gaoyang geothermal field.
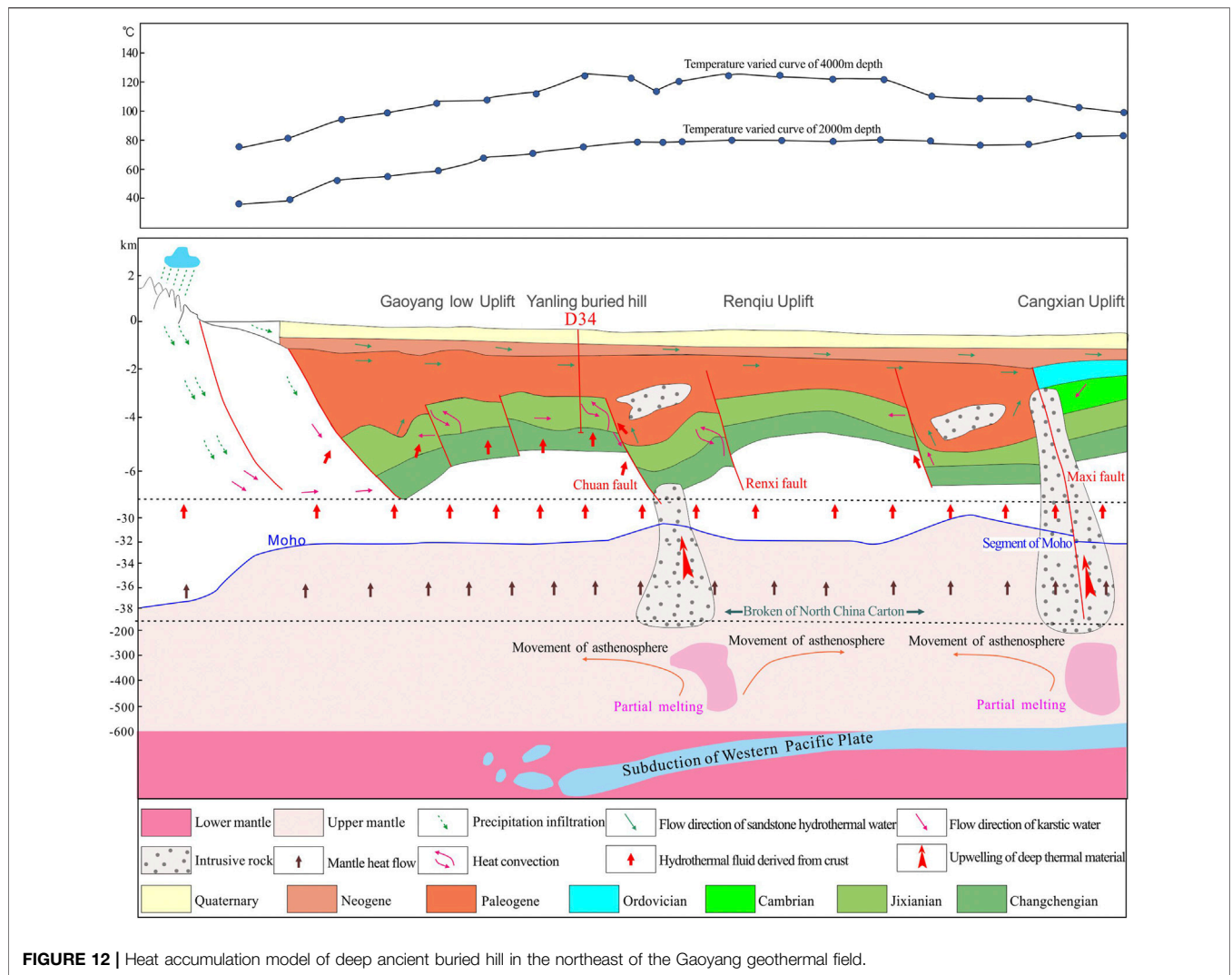
mantle. When it reached to the top of the upper mantle, the super-crust faults (such as the Maxi fault) invaded into the crust. As a result, hydrous minerals in the top of the upper mantle and the lower crust dehydrated to produce fluids intruding into the crust with the deep magma. The thickness of the Cenozoic depression around the study area can reach up to 5,000–10,000 m, and the temperature is at 130–300°C at the bottom, which make it a stable source for continuous heating of the carbonate reservoirs in the Gaoyang geothermal field. Under the effect of "thermal refraction," the heat flow accumulates from the depression with low thermal conductivity to the uplift with high thermal conductivity. Moreover, large-scale intrusive rocks with high thermal conductivity in some sections also contribute to heat flow. Meanwhile, the groundwater is heated by deep cycle and convection along the Chuan fault, and the confluence area of regional karst groundwater also has a certain heat accumulation effect. Under the influence of these favorable factors, the Gaoyang medium-temperature carbonatite geothermal field was formed.

5 CONCLUSION

Combining deep geological structure and geodynamic processes in the deep lithosphere, this article discusses the heat accumulation mechanism and the development and utilization potential of geothermal resources in the Gaoyang medium-temperature carbonatite geothermal field.

1) The thermal reservoirs in the northern Gaoyang geothermal field are the Jixian Wumishan Formation, the Gaoyuzhuang Formation, and the Cambrian–Ordovician reservoir in the south. The fractured karst and karst fractures of the Jixian carbonate reservoir are relatively developed, and aquifers account for about 20% of the stratum. As for the carbonate reservoir in the geothermal field, its buried depth is generally 3,000–4,000 m; its geothermal temperatures at the top and in the middle are 95–115°C and 110–135°C, respectively. The total flow of steam–water mixture in a single well is 234.59–331.92 t/h, the steam flow is 4.51–4.76 t/h, the

dryness is 1.36–2.03%, and the single-well power generation potential is 2.10–2.55 MW.

2) The westward subduction of the Pacific plate caused obvious damage to the eastern NCC and great reduction to the thickness of lithosphere and crust, which promote the conduction of mantle-derived heat to the shallow crust. Deep strike-slip faults such as the Maxi fault cut through the lithosphere facilitate the deep mantle-derived heat and deep magma intruding into the crust. Besides, the heat flow accumulates from the depression with low thermal conductivity to the uplift with high thermal conductivity. Groundwater is heated by deep cycle and convection along the Chuan fault, and the confluence area of the regional karst groundwater also has a certain heat accumulation effect. The Cenozoic with a thickness of more than 3,000 m and good thermal insulation effect in the Gaoyang geothermal field are favorable factors for the high temperature of the bedrock thermal reservoir. Under the influence of these factors, the Gaoyang medium-temperature carbonatite geothermal field was formed.

DATA AVAILABILITY STATEMENT

The raw data supporting the conclusion of this article will be made available by the authors, without undue reservation.

REFERENCES

Bullard, E. C., and Schonland, B. F. J. (1939). Heat Flow in South Africa. *Proc. R. Soc. Lond. Ser. A. Math. Phys. Sci.* 173 (955), 474–502.

Chen, M. X. (1992). Advances of Studies of Geothermal Resources in China. *Adv. Earth Sci.* 7 (3), 9–14.

Chen, M. X. (1988). *Geothermal in North China*. Beijing: Science Press.

Chen, M. X., Huang, G. S., Zhang, W. R., Zhang, R. Y., and Liu, B. Y. (1982). The Temperature Distribution Pattern and the Utilization of Geothermalwater at Niutuozhen Basement Protrusion of Central Hebei Province. *Sci. Geol. Sin.* 17(3), 239–252.

Dahlstrom, C. D. A. (1970). Structural Geology in the Eastern Margin of the Canadian Rocky Mountain. *Bull. Can. Petroleum Geol.* 18, 332–406. doi:10.35767/gscpgbull.18.3.332

Dai, J. X., Song, Y., Dai, C. S., Chen, A. F., Sun, M. L., and Liao, Y. S. (1995). *Inorganic Gas and its Reservoir Forming Conditions in Eastern China*. Beijing: Science Press.

Dai, M. G., Lei, H. F., Hu, J. G., Guo, X. F., Ma, P. P., and Zhang, J. Y. (2019). Evaluation of Recoverable Geothermal Resources and Development Parameters of Mesoproterozoic Thermal Reservoir with the Top Surface Depth of 3500 M and Shallow in Xiong'an New Area. *Acta Geol. Sin.* 93 (11), 2874–2888. doi:10.1111/1755-6724.13979

Faulds, J. E., and Varga, R. J. (1998). "The Role of Accommodation Zones and Transfer Zones in the Regional Segmentation of Extended Terranes,". Geological Society of America Special Paper in *Accommodation Zones and Transfer Zones: Regional Segmentation of the Basin and Range Province*. Editors J. E. Faulds and J. H. Stewart, 323, 1–46. doi:10.1130/0-8137-2323-x.1

He, L. J., and Qiu, N. S. (2014). Heating and Craton Destruction. *Chin. J. Geol.* 49 (3), 728–738. doi:10.3969/j.issn.0563-5020.2014.03.002

Lin, W. J., Wang, G. L., Gan, H. N., Wang, A. D., Yue, G. F., and Long, X. T. (2021). Heat Generation and Accumulation for Hot Dry Rock Resources in the Igneous Rock Distribution Areas of Southeastern China. *Lithosphere* 2021 (Special 5), 2039112. doi:10.2113/2022/2039112

AUTHOR CONTRIBUTIONS

FUNDING

ACKNOWLEDGMENTS

Lin, W., Wang, G., Zhang, S., Zhao, Z., Xing, L., Gan, H., et al. (2021). Heat Aggregation Mechanisms of Hot Dry Rocks Resources in the Gonghe Basin, Northeastern Tibetan Plateau. *Acta Geol. Sin. Eng.* 95 (6), 1793–1804. doi:10.1111/1755-6724.14873

Ling, M.-X., Li, Y., Ding, X., Teng, F.-Z., Yang, X.-Y., Fan, W.-M., et al. (2013). Destruction of the North China Craton Induced by Ridge Subductions. *J. Geol.* 121, 197–213. doi:10.1086/669248

Ling, M.-X., Wang, F.-Y., Ding, X., Hu, Y.-H., Zhou, J.-B., Zartman, R. E., et al. (2009). Cretaceous Ridge Subduction along the Lower Yangtze River Belt, Eastern China. *Econ. Geol.* 104, 303–321. doi:10.2113/gsecongeo.104.2.303

Liu, G. D., and Liu, C. Q. (1982). Crust and Upper Mantle Tectonics in Northern North China and Their Relationship with Cenozoic Tectonic Activity. *Sci. China Ser. B* 12 (12), 1132–1140.

Liu, G. D., Shi, S. L., and Wang, B. J. (1984). The High Conductive Layer in the Crust of North China and its Relationship with Crustal Tectonic Activity. *Sci. China Ser. B* 14 (9), 839–848.

Lu, K. Z., Qi, J. F., Dai, J. S., Yang, Q., and Tong, H. M. (1997). *Structural Model of Cenozoic Petroliferous Basin in Bohai Bay*. Beijing: Geological Publishing House, 1–251.

Mao, X. P. (2019). Characteristics of Temperature Distribution and Control Factors in Geothermal Field. *Acta Geol. Sin. Ed.* 92 (2), 96–98. doi:10.1111/1755-6724.14209

Mao, X. P. (2018). Genetic Mechanism and Distribution Characteristics of High Temperature Anomaly in Geothermal Field. *Acta Geosci. Sin. Ed.* 39 (2), 216–224. doi:10.3975/cagsb.2018.012201

Morgan, P. (1984). The Thermal Structure and Thermal Evolution of the Continental Lithosphere. *Phys. Chem. Earth* 15 (12), 107–193. doi:10.1016/0079-1946(84)90006-5

Morley, C. K., Nelson, R. A., and Patton, T. L. (1990). Transfer Zones in the East African Rift System and Their Relevance to Hydrocarbon Exploration in Rifts. *AAPG Bull.* 74, 1234–1253. doi:10.1306/0c9b2475-1710-11d7-8645000102c1865d

Pang, J. M., Pang, Z. H., Lv, M., Tian, J., and Kong, Y. L. (2018). Geochemical and Isotopic Characteristics of Fluids in the Niutuozhen Geothermal Field, North China. *Environ. Earth Sci.* 77 (1), 12.1–12.21. doi:10.1007/s12665-017-7171-y

Pang, Z. H., Kong, Y. L., Pang, J. M., Hu, S. B., and Wang, J. Y. (2017). Geothermal Resources and Development in Xiongan New Area. *Bull. Chin. Acad. Sci.* 32 (11), 1224–1230.

Qi, J. F. (2007). Structural Transfer Zones and Significance for Hydrocarbon Accumulation in Rifting Basins. *Mar. Orig. Pet. Geol.* 12 (4), 43–50. doi:10.3969/j.issn.1672-9854.2007.04.007

Qi, J. F. (2004). Two Tectonic Systems in the Cenozoic Bohai Bay Basin and Their Genetic Interpretation. *Geol. China* 31 (1), 15–22.

Wang, G. L., Li, J., Wu, A. M., Zhang, W., and Hu, Q. Y. (2018). A Study of the Thermal Storage Characteristics of Gaoyuzhuang Formation, A New Layer System of Thermal Reservoir in Rongcheng Uplift Area, Hebei Province. *Acta Geosci. Sin.* 39 (5), 533–541. doi:10.3975/cagsb.2018.071901

Wang, G. L., and Lin, W. J. (2020). Main Hydro-Geothermal Systems and Their Genetic Models in China. *Acta Geol. Sin.* 94 (7), 1923–1937. doi:10.1111/1755-6724.14469

Wang, G. L., Zhang, W., Lin, W. J., Liu, F., Zhu, X., Liu, Y. G., et al. (2017). Research on Formation Mode and Development Potential of Geothermal Resources in Beijing-Tianjin-Hebei Region. *Geol. China* 44 (6), 1074–1085. doi:10.12029/gc20170603

Wang, J. Y., Pang, Z. H., Hu, S. B., He, L. J., Hang, S. P., and Qiu, N. S. (2015). *Geothermics and its Applications*. Beijing: Science Press.

Wang, P. X., Yang, X., and Bian, X. D. (2012). Petrologic and Geochemical Characteristics of Igneous Rock in Jizhong Depression. *Geol. Sci. Technol. Inf.* 31 (4), 4–13.

Wang, S., Zhang, H. D., Sun, J. C., Guo, G. P., Jing, J. H., and Tian, G. S. (2010). *Modeling of Formation and Evolution of Deep Water and Hydrocarbon Migration and Accumulation in the Basin*. Beijing: Geological Publishing House.

Wang, S. Q., Zhang, B. J., Li, Y. Y., Xing, Y. F., Yuan, W. Z., Li, J., et al. (2021). Heat Accumulation Mechanism of Deep Ancient Buried Hill in the Northeast of Gaoyang Geothermal Field, Xiong'an New Area. *Bull. Geol. Sci. Technol.* 40 (3), 12–21. doi:10.19509/j.cnki.dzkq.2021.0319

Wang, Z., Gao, P., Jiang, G., Wang, Y., and Hu, S. (2021). Heat Flow Correction for the High-Permeability Formation: A Case Study for Xiong'an New Area. *Lithosphere* 2021 (Special 5), 9171191. doi:10.2113/2021/9171191

Wu, A. M., Ma, F., Wang, G. L., Liu, J. X., Hu, Q. Y., and Miao, Q. Z. (2018). A Study of Deep-Seated Karst Geothermal Reservoir Exploration and Huge Capacity Geothermal Well Parameters in Xiongan New Area. *Acta Geosci. Sin.* 39 (5), 523–532. doi:10.3975/cagsb.2018.071104

Xia, Q.-K., Liu, J., Liu, S.-C., Kovács, I., Feng, M., and Dang, L. (2013). High Water Content in Mesozoic Primitive Basalts of the North China Craton and Implications on the Destruction of Cratonic Mantle Lithosphere. *Earth Planet. Sci. Lett.* 361, 85–97. doi:10.1016/j.epsl.2012.11.024

Xia, Q. L., Tian, L. X., Zhou, X. H., Wang, Y. B., Yu, Y. X., and Lu, D. Y. (2012). *Tectonic Evolution and Deformation Mechanism of Bohai Sea Area*. Beijing: Petroleum Industry Press.

Xiao, S. B., Gao, X. L., Jiang, Z. X., and Qiao, H. S. (2000). Cenozoic Dextral Strike-Slip Motion in Bohai Bay Basin and its Meaning to Petroleum Geology. *Geotect. Metallogenia* 24 (4), 321–328. doi:10.3969/j.issn.1001-1552.2000.04.004

Xiong, L. P., and Gao, W. A. (1982). Characteristics of Geotherm in Uplift and Depression. *Chin. J. Geophys.* 25 (5), 60–68.

Xiong, L. P., and Zhang, J. M. (1984). Mathematical Simulation of Refraction and Redistribution of Heat Flow. *Chin. J. Geol.* 19 (4), 445–454.

Xu, C. F. (2003). Lithospheric Structure, Basin Structure and Hydrocarbon Migration in Mainland China. *Earth Sci. Front.* 10 (3), 115–127.

Xu, J., Han, Z. J., Wang, C. H., and Niu, L. F. (1996). Preliminary Study on Two Newly-Generated Seismotectonic Zones in North and Southwest China[J]. *Earthq. Research China* 10 (4), 393–401.

Yan, D. S., and Yu, Y. T. (2000). *Evaluation and Utilization of Geothermal Resources in Beijing Tianjin Hebei Oil Region*. Wuhan: China University of Geosciences Press.

Yang, M. H. (2009). Transfer Structure and its Relation to Hydrocarbon Exploration in Bohai Bay Basin. *Acta Pet. Sin.* 30 (6), 816–823. doi:10.3321/j.issn:0253-2697.2009.06.004

Yue, G. F., Wang, G. L., and Ma, F. (2020). The State and Convergence Mechanism of Geothermal Energy in the Buried Hills in Xiong'an New Area. *Geotherm. Energy* (2), 14–19.

Zhang, B. J., Gao, Z. J., Zhang, F. Y., Hao, S. H., Liu, F. Y., and Zang, J. J. (2015). Hydrodynamic Condition and Response of Formation Water Chemical Fields of Geothermal Water in North China Basin. *Earth Sci. Front.* 22 (06), 217–226. doi:10.13745/j.esf.2015.06.017

Zhang, B. J., Li, Y. Y., Gao, J., Wang, G. L., Li, J., Xing, Y. F., et al. (2020). Genesis and Indicative Significance of Hot Dry Rock in Matouying, Hebei Province. *Acta Geol. Sin.* 94 (7), 2036–2051. doi:10.19762/j.cnki.dizhixuebao.2020226

Zhang, Y. Q., Shi, W., and Dong, S. W. (2019). Neotectonics of North China: Interplay between Far-Field Effect of India- Eurasia Collision and Pacific Subduction Related Deep-Seated Mantle Upwelling. *Acta Geol. Sin.* 93 (5), 971–1001. doi:10.1111/1755-6724.14187

Zhu, R., and Xu, Y. (2019). The Subduction of the West Pacific Plate and the Destruction of the North China Craton. *Sci. China Earth Sci.* 62, 1340–1350. doi:10.1007/s11430-018-9356-y

Zuo, Y. H., Qiu, N. S., ChangHao, J. Q. Q., Li, Z. X., Li, J. W., Li, W. Z., et al. (2013). Meso-Cenozoic Lithospheric Thermal Structure in the Bohai Bay Basin. *Acta Geol. Sin.* 87 (2), 145–153.

Zuo, Y., Qiu, N., Hao, Q., Zhang, Y., Pang, X., Li, Z., et al. (2014). Present Geothermal Fields of the Dongpu Sag in the Bohai Bay Basin. *Acta Geol. Sin. - Engl. Ed.* 88 (3), 915–930. doi:10.1111/1755-6724.12246